Institutionen för medicin och vård
Avdelningen för radiofysik
Hälsouniversitetet

Experimental determination of the angular dependence of the directional dose equivalent, H'(d), for ISO "narrow" X ray fields and ^{137}Cs γ-rays measured in a PMMA sphere and a PMMA slab phantom

Eva Lund, Frantisek Pernicka, and Carl A Carlsson

Department of Medicine and Care
Radio Physics
Faculty of Health Sciences

Series: Report / Institutionen för radiologi, Universitetet i Linköping; 76
ISSN: 1102-1799
ISRN: LIU-RAD-R-076

Publishing year: 1993

© The Author(s)

Experimental determination of the angular dependence of the directional dose equivalent, H'(d), for ISO "narrow" X ray fields and ^{137}Cs γ-rays measured in a PMMA sphere and a PMMA slab phantom.

Lund Eva[1], Pernicka Frantisek[2], and Carlsson Carl A.[1]

[1] Department of Radiation Physics, Faculty of Health Sciences, Linköping University

S-581 85 Linköping, Sweden.

[2] Institute of Radiation Dosimetry, Czeckoslovak Academy of Sciences, Prague, Czeck Republic.

Abstract:

For the purpose of calibrating individual dosimeters in X-ray fields conversion factors from air kerma free in air to dose equivalent at a specified depth in a phantom have been calculated among others by Grosswendt (1991,1992). By means of Monte Carlo calculations the angular dependence factor for photon beams of oblique incidence is also studied for different phantom shapes and compositions as well as for different X-ray qualities. However, till now there has been a lack of experimental verification of the angular dependence factors.

In this investigation the conversion factor from air kerma to $H_p(10)$ has been determined for the following X-ray qualities: 40 kV, 80 kV, and 295 kV, ISO "narrow" spectra and for 137Cs γ-rays using thermoluminescent (TL) dosimeters. The angular dependence factor $H'(10,\alpha)/H'(10,0^o)$ has also been experimentally determined for the same X-ray and γ -ray qualities and for different angles between 0° and 180°.

The conversion factors are found to be in good agreement with the calculated ones for the PMMA sphere phantom, while some minor discrepancies are found between the experimental and calculated angular dependence factors for the 30x30x15cm^3 PMMA slab phantom.

The difference in angular dependence obtained for the slab and the sphere is discussed as well as the possibility to underestimate the personal dose equivalent, $H_p(10)$, compared to effective dose, E.

1. Introduction

The international Commission on Radiation Units and Measurements (ICRU) introduced in the report ICRU 39 (1985) two quantities for personal monitoring; the individual dose equivalent, penetrating $H_p(d)$ and superficial $H_s(d)$. The dose equivalents in soft tissue are defined in the ICRU sphere below a specified point on the sphere at a depth d, chosen differently for strongly penetrating radiation and for weakly penetrating radiation respectively. In a recent report ICRU 47 (1992) instead of these two quantities for individual monitoring, a simplified concept, called personal dose

equivalent, $H_p(d)$, is introduced that is appropriate for both strongly and weakly penetrating radiation, depending on the value of the depth, d.

This operational quantity, the personal dose equivalent, is based on the concept of the dose equivalent at a point and not on the concept of equivalent dose for an organ as defined in ICRP 60. Furthermore this quantity is expected to give reasonable approximation of the effective dose and the equivalent dose to the skin for beam qualities with the quality factor Q(L) = 1 (ICRP 60, 1991)

The quantity $H_p(10)$ can be measured with the dosimeter worn on the trunk or elsewhere on the surface of the body. The dosimeters must be calibrated under well-known standard conditions such as the radiation quality of the reference field, the irradiation geometry and using an appropriate phantom. According to ICRU (ICRU 33,1980) a 30 cm diameter tissue-equivalent sphere with a density of 1 $g \cdot cm^{-3}$ is a good approximation of the human trunk considering backscattered radiation. In practice the calibration might be performed in a parallel beam on the ICRU sphere in terms of the directional dose equivalent, H'(d,α), i.e. the dose equivalent at d mm depth below the point of the surface where the dosimeter is fixed. The direction is specified by the angle between the radius, where the center of the dosimeter is located and the direction of the incident parallel beam, see Fig 1.

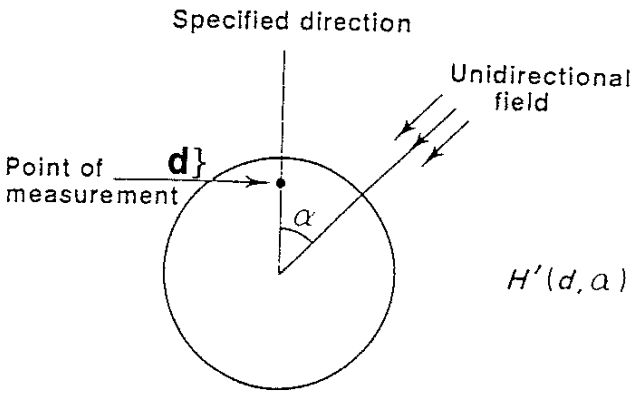

Fig 1 Definition of the angle of incidence α for H'(d,α).

Since a primary standard for the directional dose equivalent does not exist reference has to be made to metrologically representable quantities such as air kerma, with recourse to conversion factors for converting these quantities to the directional dose equivalent.

The sphere is however a rather impractical phantom if many dosimeters are to be calibrated. It is difficult to fabricate a phantom with this shape and to find an exact substitute for the 4 element ICRU composition. In the time period since 1985 different kinds of phantoms have been used as for instance spheres in PMMA (polymethyl methacrylate), cube phantoms in water (IAEA 1988), and slab phantoms in PMMA (Wernli et al 1989) (in order to give calibration results within the guidelines given by

ICRU. It is nevertheless desirable to achieve uniformity in the calibration procedure, therefore a PMMA slab phantom 30x30x15cm^3 is recommended as a substitute for the ICRU sphere.(ICRU 47,1992).

The present investigation was proposed by the Swedish National Institute of Radiation Protection,SSI, in order to design and test a calibration procedure for individual dosemeters with the new operational quantities for the radiation protection in Sweden. The main purpose was to verify the calculated angular dependence of the directional dose equivalent H'(10,α) which for an aligned and expanded radiation field is equivalent to $H_p(10)$ when determined in the ICRU sphere. The experiments started with determinations of H'(10,α) in a PMMA sphere with a diameter of 30 cm for different angles from 0° - 180° and for different radiation qualities: ISO "narrow" field 40 kV, 80kV and 295 kV as well as ^{137}Cs γ-field.(ISO 1979)

During the course of the work the difficulties in fabrication of spherical phantoms as well as the possibilities to calibrate more than one dosimeter at the same time was noticed. Different shapes and materials for test phantoms have been used and Grosswendt (1991, 1992) has published calculated conversion factors for air kerma to H'(10, α) for different beam qualities and phantom materials as well as for normal and oblique incidence at different angles of a broad parallel beam. In order to confirm the calculated angular dependence we repeated the measurements for a 30x30x15cm^3 PMMA slab .

The calculated conversion factors for normal incidence, air kerma to H'(10, 0°) are experimentally confirmed by ourselves and recently by Will (1991).

The measurements reported here are performed with the same equipment and in the same environment as the Swedish standard calibrations will be done, thus taking into account local variations.

In the recent ICRU 47 (1992) report the accuracy requirements for determination of dose equivalent are discussed. In most cases an overall uncertainty of one standard deviation of 30 % should be acceptable. The ICRP publication 35 (ICRP 35) has provided a statement that is generally consistent with this limit. It requires that the uncertainty in the measurement of the annual value of the corresponding quantities is reduced as far as reasonably achievable, but if the dosimetric quantities are of the order of the relevant annual limits the uncertainty should not exceed one standard deviation of 25 %. The requirements are less demanding when the doses per year are less than 10 mSv.

2.Experimental equipment

2.1 Photon sources

Conversion factors are deduced from measurements in the ISO narrow X-ray fields; 40 kV, 80 kV and 295 kV and in a ^{137}Cs photon field.

The X-ray beams were generated by a high precision power supply unit Pantac HF 420 C and a ceramic X-ray tube with an equivalent window thickness of 7 mm Be (AEG type MB 42011). The additional filtration satisfied the purity and thickness requirements given in the ISO 4037 report. The anode angle is 20°.

The X-ray machine was highly stabilized with a short term repeatability for both voltage and current of better than 0.01 %.

The ^{137}Cs source used for this experiment was the " GBq source" at the dosimetric standard laboratory.

2.2 Calibration phantoms

The ICRU soft tissue is a hypothetical material and it is hard to find a material with the same composition (76.2 % O, 11.1 % C, 10.1% H and 2.6 % N by weight). Various alternative phantom types are in use. Water is an excellent substitute for these radiation energies but must be encapsulated in some non tissue equivalent material. Perroche and Bouttillon (1989) used water within a 3 mm thick spherical shell of PMMA . We have instead made the whole sphere of PMMA.

Because of the impractical shape of the sphere for calibration of more than one personal dosemeter, IAEA, for instance, applied a cuboid water phantom,(IAEA 1988) edge length 30 cm. Since ICRU gave more preference to the PMMA slab phantom $30x30x15cm^3$ (ICRU 47) we have chosen this phantom type for our determinations.

Both phantoms are equipped with a special slide for carrying thermoluminescent, TL, dosimeters at a certain depth corresponding to 10 mm in a material with the proposed density of 1.0 g/cm^3.

2.3 Dosimeters

Extruded thermoluminescent tablets with 4.5 mm diameter and 0.8 mm thick were used as dosemeters for the measurements. We mainly used LiF(Mg, Ti) as dosemeter material, but also $Li_2B_4O_7$(Mn) was used for test measurements since this material is more equal to PMMA and tissue than LiF.

A relative calibration of the individual dosemeters was repeated six times resulting in an individual spread in sensitivity of less than 2 %, one standard deviation. All dosemeters passed the same thermal treatment before and after every irradiation. For

LiF the dosemeters were annealed for 1 h in 400°C and 24 h in 80°C and preheated immediately before read-out, 20 min in 80°C. This treatment sequence was carefully kept for all measurements in order to avoid sensitivity changes in the dosemeters caused by different delay periods between irradiation and read out. The automatic DOSACUS[1] TL-reader was used for the read out.

3. Experimental procedure

3:1 Irradiation geometry

The phantoms were irradiated at a distance of 2 m from the X-ray tube anode and the center of the ^{137}Cs source respectively. Without external collimating the beam is broad enough to irradiate the whole sphere when it is centered in the beam. As demanded for the definition of the directional dose equivalent H'(d,α) the radiation field should be expanded, i e, the fluence and its angular and energy distributions should be the same throughout the volume of interest. In order to fulfill this the irradiations were performed with the phantom rotated so that the dosimeter position always was in the center of the beam (Fig 3b). In a true expanded field H'(d,α) could be measured for all directions in one single irradiation, see Fig 4a. The practical solution of the rotation of the phantoms is shown in Fig 2.

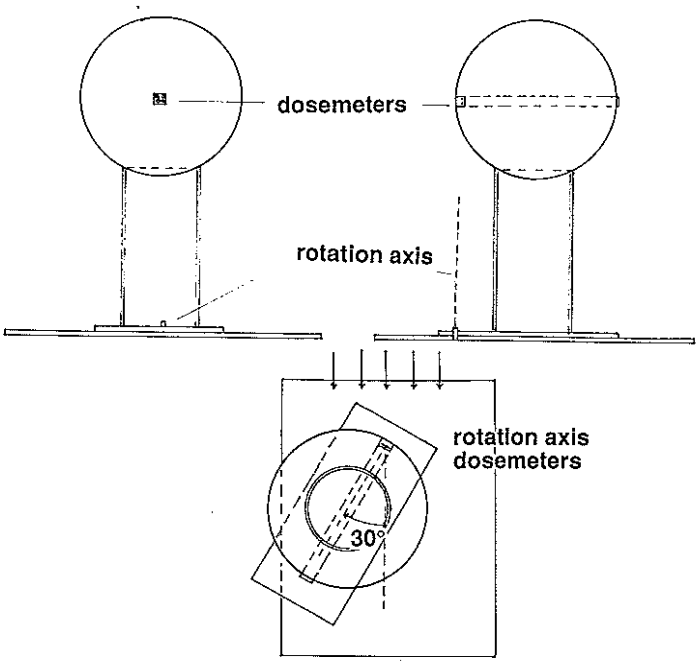

Fig 2 The phantom, its cylindrical support and a PMMA plate are fixed together and are possible to rotate simultanously around a vertical axis through the position of the TL dosemeters. With this technique the dosemeters are always in the center of the radiation field at a specified distance from the radiation source.

1) DOSACUS , Alnor instruments.

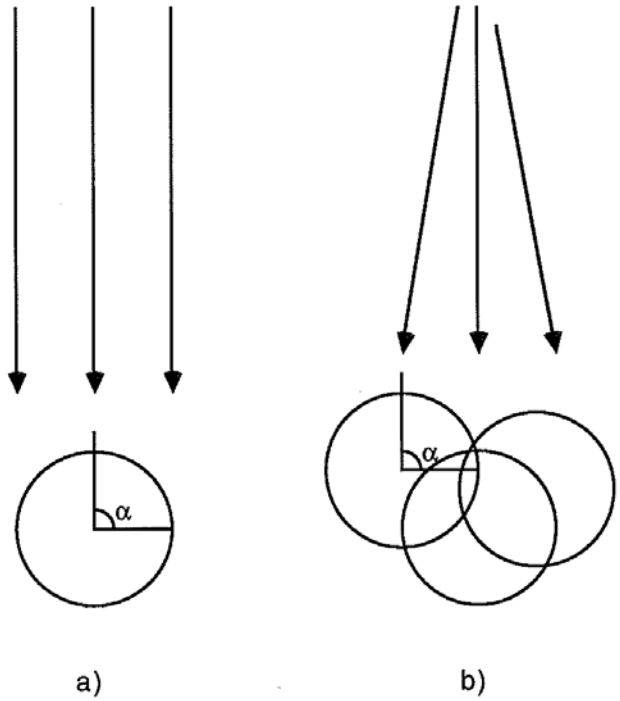

Fig 3. a) H'(d,α) can be determined for all α in the same irradiation if the radiation field is broad and parallel, b) The sphere is rotated so that the dosimeters are in the same position independent of the angle and thus in the same expanded, radiation field for all angles α For all orientations of the sphere, the primary radiation is equal at the position of the dosemeters in both geometries, any differences should be due to various scatter contributions to the dosemeters.

From theories of conversion of depth doses from one source to surface distance to another (Burns 1958, Johns 1958) it has been concluded that the scatter contribution to the absorbed dose in a point at a certain depth depends on the field area at this depth and not on the divergence of the beam. In the case of a spherical phantom we may assume that the curvature of the surface is small and might be regarded as plane, see Fig 4.

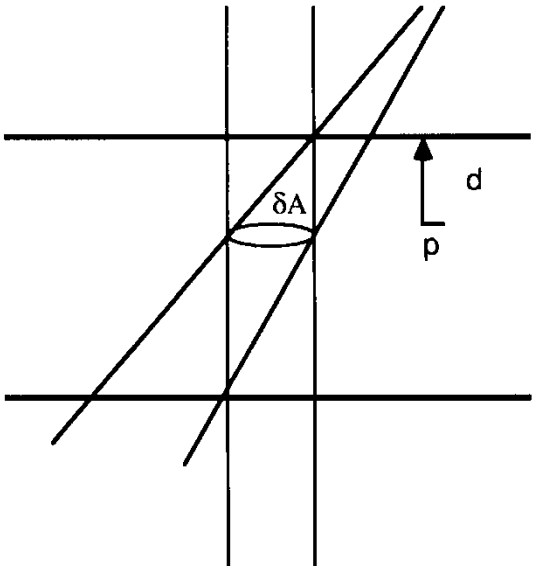

Fig 4 The scatter contribution to the absorbed dose in the point P at a depth d from the beam with cross section δA, is approximately independent of the divergence of the beam.

Since the contributions from primary as well as scattered radiation to the absorbed doses in the dosimeters are approximately equal, the both geometries in fig 4 are for our purpose equivalent.

3.2 Field area problems.

Our choice of geometry means that H' (10,α) can be determined as in an expanded field. In practice however, this choice of geometry requires a field diameter of 600 mm if the sphere should be completely within the radiation field even at directions around

$\alpha = 90^{o}$. The demands on the field area could not be fulfilled at 2 m distance from the anode as shown from X-ray images obtained with the sphere in 4 different positions, see Fig 5. In most directions the sphere is only partly irradiated. In the case of irradiation with ^{137}Cs the sphere was within the radiation field for all angles of incidence.

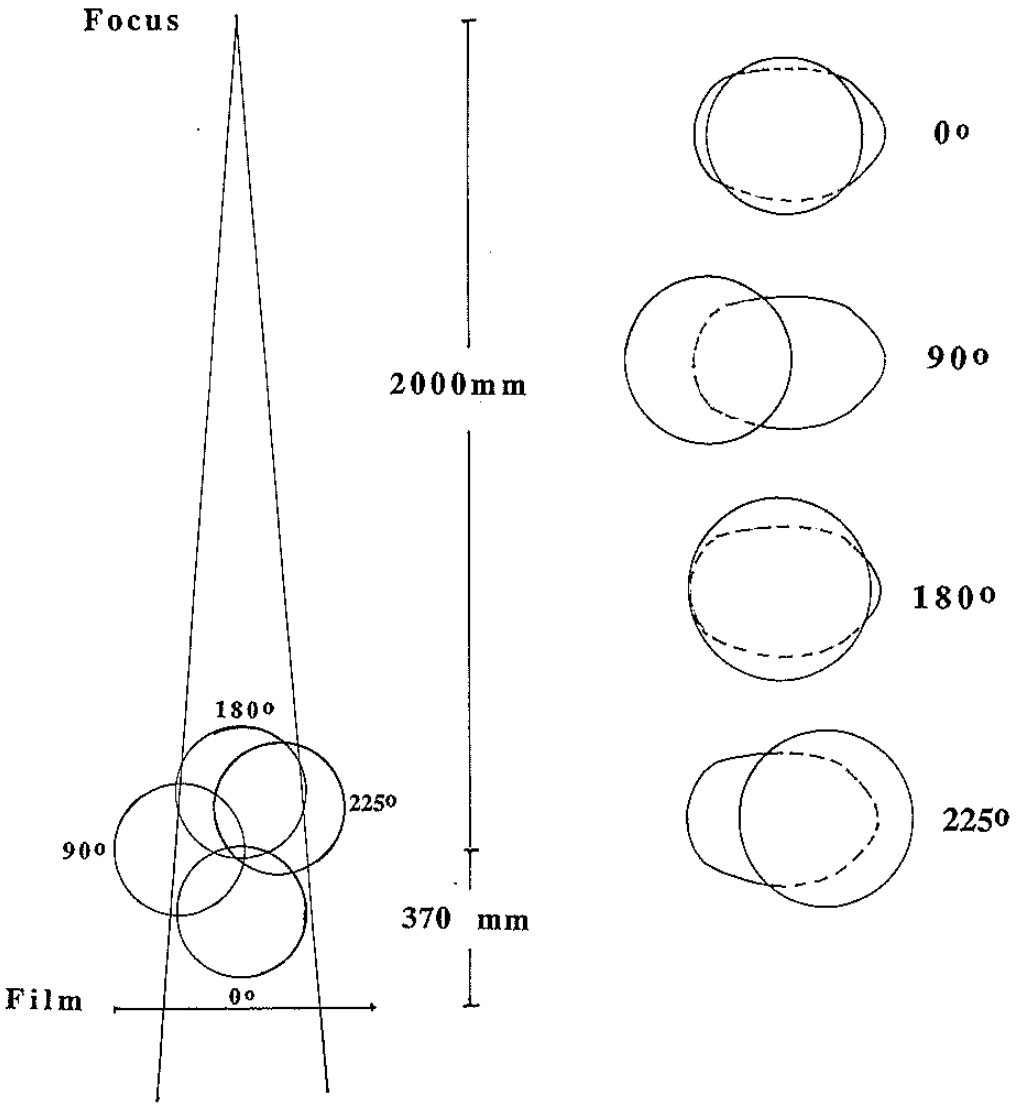

Fig 5: The geometry for the X-ray irradiation with actual field size and the sphere rotated 0°, 90°, 180°, and 270°. b) Projections of the field and sphere on the film.

Another problem is the inhomogeneity in an X-ray field caused by the anode angle. This so called heel-effect in the anode-cathode direction causes variations in both fluence and the energy spectrum of the photons over the field. The anode angle is 20° for the X-ray tube used in this experiment. The homogeneity measured as air kerma has been determined centrally in the anode cathode direction as well as perpendicular to this direction and the variation was found to be +/- 10 %. The dosimeters are always situated in the center of the beam and the variations due to the heel effect did not affect the amount of backscatter from the phantom. The detector signal was found to be the same

within the obtained accuracy,when the phantom was irradiated with an angle of incidence of 90 ^{o} as when it was rotated to 270°.

3.3.1 Theory

The dosimeters are 4.5 mm in diameter and 0.8 mm thick and for photon energies below 300 keV charged particle equilibrium, CPE, is assumed to be established both when they are irradiated free in air and inside the PMMA phantom. The collision kerma in the TL material can be calculated from:

$$K_{c,TL} = \left(\frac{\overline{\mu}_{en}}{\rho}\right)_{air}^{TL} K_{c,air} \qquad (1)$$

The average mass energy absorption coefficient for the two materials is obtained from:

$$\frac{\overline{\mu}_{en}}{\rho} = \int_0^\infty \frac{\mu_{en}(h\nu)}{\rho} \Psi_{h\nu} \frac{1}{\Psi} d(h\nu) = \frac{K_c}{\Psi}$$

$$K_c = \int_0^\infty \frac{\mu_{en}(h\nu)}{\rho} \Psi_{h\nu} d(h\nu) \qquad (2)$$

Since CPE is assumed to be established, the average absorbed dose in the dosemeter is approximately equal to collision kerma:

$$\overline{D_{TL}} \approx \overline{K}_{c,TL} = \int_0^\infty \frac{\mu_{en}(h\nu)}{\rho} \Psi_{h\nu} d(h\nu)$$

$$or \qquad (3)$$

$$\overline{D_{TL}} \approx \overline{\left(\frac{\mu_{en}}{\rho}\right)}_{air}^{TL} K_{c,air}$$

Collision kerma K_c is approximately equal to kerma K for energies below 1 MeV for low-Z materials like air and the TL material since the bremsstrahlung losses are negligible. The light signal, M, emitted by the TL dosemeters is assumed to be proportional to the mean absorbed dose in it.

The response of the dosemeter, n_c is defined as the signal per unit air collision kerma. If n_c is normalized to the response for 1.25 MeV photons the energy dependence can be expressed as:

$$\frac{n_{c,h\nu}}{n_{c,^{60}Co}} = \frac{\dfrac{M_{h\nu}}{K_{c,air}(h\nu)}}{\dfrac{M_{^{60}Co}}{K_{c,air}(^{60}Co)}} = \frac{\eta_{h\nu}\left[\dfrac{\overline{\mu}_{en}}{\rho}\right]^{TL}_{air,h\nu}}{\eta_{^{60}Co}\left[\dfrac{\overline{\mu}_{en}}{\rho}\right]^{TL}_{air,^{60}Co}} \tag{4}$$

$$M_{h\nu} = \eta_{h\nu} \cdot \left(\frac{\mu_{en}}{\rho}\right)^{TL}_{air} \cdot K_{c,air} = n_{c,h\nu} \cdot K_{c,air} \tag{5}$$

Here c in n_c stands for calibration free in air; η, is the signal per unit absorbed dose in the dosemeter. The energy response of the TL dosemeters were experimentally determined for a number of beam qualities covering "narrow" X-ray spectra with effective energies from 28 keV to 242 keV as well as 662 keV and 1.25 MeV from ^{137}Cs and ^{60}Co respectively. The result is shown in Table 1 and Fig. 6. The effective energy is here defined as the energy that has the same air- kerma HVL as the spectrum.

3.3.2 Measurements

The response of the TL-dosemeters was determined by measuring their signal after irradiation free in air.The dosemeters were placed in a paperholder at a distance of 1 m from the photon source. During the measurements the dosemeters were irradiated at different angles of incidence. This did not affect the response for photon energies above about 30 keV. At an angle of incidence α the detecting area is decreased by a factor of cos α which is compensated by longer track length in the dosemeter, increased by a factor of 1/cos α For lower energies this compensation is not fulfilled because of attenuation in the dosemeter material. For gamma energies above 300 keV the dosemeters were covered by teflon in the case of LiF and by the detector material itself for $Li_2B_4O_7$ in order to establish charged particle equilibrium in the dosemeter.

Table I :The response of the Li F dosemeters normalized to ^{60}Co gamma rays and compared with results for TL-100* from da Rosa et al (1988) and the $(\mu_{en}/\rho)_{TL,air}$ratio. The energy response is determined for a series of "narrow" X-ray spectra characterized by number and effective energy

No	E_{eff} keV	K_{air} mGy	n_k digit/μGy	$n_{c,hv}/n_{c,Co-60}$	TLD-100*	$(\mu_{en}/\rho)_{LiF,air}$
18	28	0.595	65.48±0.20	1.448±0.042	1.376	1.279
9	32	8.67	65.13±0.32	1.425±0.015	1.375	1.276
10	46	13.54	59.76±0.60	1.319± 0.027	1.341	1.218
11	64	6.87	59.20±1.00	1.278± 0.024	1.275	1.166
12	82	4.12	54.88± 0.33	1.194± 0.015	1.216	1.087
13	103	4.71	52.59± 0.49	1.151± 0.013	1.159	1.034
14	120	34.08	51.61± 0.81	1.129± 0.017	1.122	1.023
15	155	11.26	49.97± 1.30	1.093± 0.020	1.065	1.010
16	198	10.69	49,58± 0.45	1.085± 0.015	1.021	1.005
17	242	10.57	48.15± 0.60	1.053±0.011	0.993	1.004
137Cs	662	21.15	45.71±0.15	1.000±0.011	0.960	0.992
60Co	1250	6.265	45.71±0.45	1.000±0.010	1.000	1.000

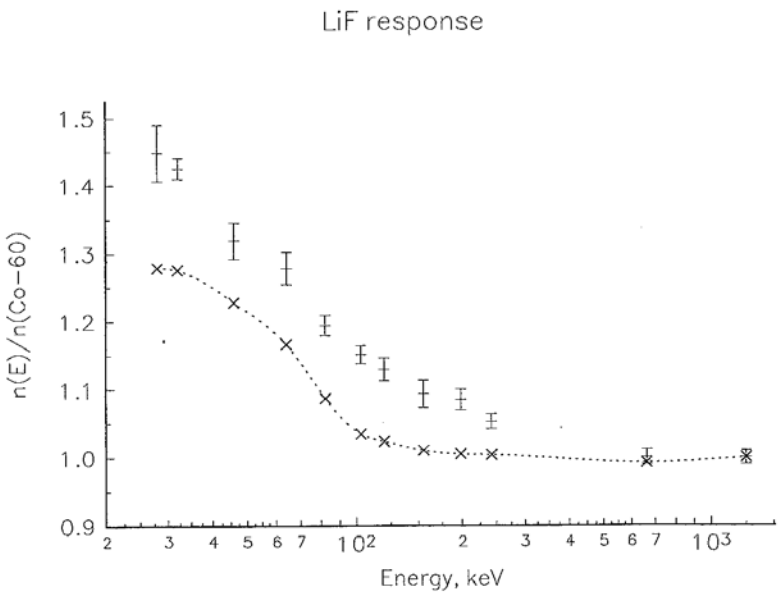

Fig 6: The response of the LiF-dosemeters as a function of effective energy of the X-ray spectra and normalized to ^{60}Co γ-rays. The dotted curve is the $(\mu_{en}/\rho)_{LiF,\ air}$ ratio as a function of energy.

4.Experimental results

4.1 Measurements of $H'(10,0^o)/K_{air}$

Calculated values of the conversion factor $H'(10,0^o)/K_{air}$ have been published by several authors (Bartlett et al 1989,Grosswendt 1989, 1990, 1991) These values are mainly based on Monte Carlo calculations for both gamma mono energies and for X-ray spectra incident normally to the ICRU sphere or other phantoms. The theoretical values have been verified experimentally for a cuboid waterphantom (Will, W 1989) and a PMMA slab phantom (Will ,W1991).

The present measurements of $H'(10,0^o)/K_{air}$ (free in air) were carried out at a distance of 1 m, with the PMMA phantoms. Four TL-dosemeters were positioned in the center of the beam inside the phantom at a depth corresponding to 1.0 g/cm^2 giving an average signal M_p. The average signal from four other dosemeters was registered after irradiation free in air, M_{air}.

We now have:

$$\frac{M_{air}}{\eta_{hv}} = K_{air}\left(\frac{\overline{\mu}_{en}}{\rho}\right)_{air}^{LiF} \qquad (6)$$

$$\frac{M_p}{\eta_{hv,p}} = K_{air,p}\left(\frac{\overline{\mu}_{en}}{\rho}\right)_{p,air}^{LiF}$$

$$\frac{K_{air,p}}{K_{air}} = \frac{M_p}{M_{air}}\left(\frac{\overline{\mu}_{en}}{\rho}\right)_{air}^{air,p}$$

Here, K_{air} and $K_{air,p}$ are the values of air kerma free in air and inside the phantom at the point of measurement, respectively.

If we assume the energy response of the dosemeters to be the same free in air as inside the phantom $\left(\frac{\overline{\mu}_{en}}{\rho}\right)_{air}^{air,p}$ will be equal to 1. That means that the energy spectrum inside the phantom is not allowed to result in an effective energy differing so much from the primary spectrum that the energy response of the TL tablet will change. By means of Monte Carlo calculations, Fluslab, (Pernicka, 1991) the effective energy regarding the energy absorption properties is found to be 30.1 keV inside the phantom compared to 31.1 keV at the phantom surface for the ISO narrow 40 kV spectrum. Comparable results are obtained for the 80 kV spectrum while the difference is larger for the 295kV spectrum where the effective energy at the surface is 180 keV and at a depth of 1.0 g/cm^2 169 keV. In this energy region, however, the dosemeter response varies very slowly with energy and we can assume that the energy response of the dosemeters are approximately the same inside the phantom as free in air even in the energy region around 200 keV. The dose equivalent in the phantom material PMMA at

a specified point inside the phantom may be determined by means of the TL dosemeters:

$$H_p(d) = D_{ph}(d) = \left(\frac{\overline{\mu}_{en}}{\rho}\right)_{LiF}^{p} \overline{D}_{LiF} \qquad (7)$$

while assuming that the quality factor, Q, for the radiation is equal to 1. The mean absorbed dose in the LiF dosemeter inside the phantom will be:

$$\overline{D}_{LiF} = \left(\frac{\overline{\mu}_{en}}{\rho}\right)_{p,air}^{LiF} K_{p,air}(d) \qquad (8)$$

If eqs 5,6 and 7 are combined and divide by K_{air}

$$\frac{H_p(d)}{K_{air}} = \frac{K_{air,p}(d)}{K_{air}}\left(\frac{\overline{\mu}_{en}}{\rho}\right)_{air}^{p} = \frac{M_p}{M_{air}}\left(\frac{\overline{\mu}_{en}}{\rho}\right)_{air}^{p} \qquad (9)$$

The conversion factor is thus simply determined from the ratio between the detector signals registered from the irradiation inside the phantom and the irradiation free in air multiplied with the ratio of the mass energy absorption coefficients for PMMA to air averaged over the spectrum of the energy fluence of photons inside the phantom.

The experimental results of the conversion factors of air kerma to the personal dose equivalent (Eq 9) is collected in Tables 2.a and b. and are compared with calculated values by Grosswendt (1988) for the sphere, and with experimental results by Will (1991), calculated values by Grosswendt (1991) and Pernicka (1991) for the slab phantom.

Table IIa. Experimental determination (this work) of the conversion factor $H'(10,0^{o})/ K_{air}$ for a PMMA sphere. The experimental values are compared with values calculated by Grosswendt (1988) for the ICRU sphere. These values are divided by k_v, a correction factor for converting air kerma on the surface of a sphere made of PMMA into air kerma on the ICRU sphere. The converted values are comparable with our experimental values for a PMMA sphere

quality	Experiment Sv/Gy	Grosswendt Sv/Gy	k_v	Grosswendt converted Sv/Gy
40 kV	1.306±0.019	1.189	0.916	1.298
80 kV	1.872±0.029	1.741	0.918	1.897
295 kV	1.404±0.012	1.357	0.979	1.386
662 keV	1.192±0.011	1.196	0.997	1.200

Table IIb Experimental determination of the conversion factor $H'(10,0^o)/K_{air}$ for the PMMA slab phantom. The experiment values are compared with experimental values from Will (1991), calculated values by Grosswendt (1992), and calculated values of Pernicka (Monte Carlo code, FLUSLAB, private communication, 1991).

.

quality	Experiment Sv/Gy	Will Sv/Gy	Grosswendt Sv/Gy	Pernicka Sv/Gy
40 kV	1.39± 0.04	1.40	1.31	1.24±0.02
80 kV	2.11±0.04	2.02	2.07	2.05±0.03
295 kV	1.42±0.03	1.45	1.47	1.46±0.02
662 keV	1.26±0.02	1.22	1.24	

4.2 Determination of the angular dependence factor $H_p(10,\alpha)/H_p(10,0^o)$.

Calculated angular dependence factors have been published for both the ICRU sphere and for the PMMA slab phantom by Grosswendt (1988, 1991, 1992). Till now no experimental verification of the calculated values has been available.

The experimental technique to measure the absorbed dose in the detector at a depth of 1 g/cm^2 at different angles of incidence has been described in sect.3.1. We make the assumption that the response of the dosemeters does not depend on the orientation of the sphere with respect to the direction of the beam, i e that the energy spectrum has not changed at the position of the detector when irradiated free in air and at a depth of 1 g/cm^2 in PMMA. This seems to be justified for the measurements in the sphere since the angular dependence has been determined by means of both LiF dosemeters and $Li_2B_4O_7$. The latter TL material is less energy dependent i e it is more equivalent to PMMA than LiF. Both experiments gave the same result.

The rotation of the phantom to obtain the correct angle of incidence for the radiation field is described in Fig 3. The relative variation with angle of incidence $H'(10,\alpha)/H'(10,0^o)$ is then given by the ratio of the signal from the dosemeters irradiated under the angle of incidence α and from those irradiated under normal incidence.

In the present investigation the angular dependence factor is determined for a PMMA sphere for angles between $0^o$and 180° for the ISO "narrow" X-ray fields : 40 kV, 80 kV and 295 kV and ^{137}Cs γ-rays. The experimental results are shown in Table 3 together with the calculated values by Pernicka (1991), Grosswendt.(1988), and Dimbylow (1988).

Table IIIa The angular dependence factor for a PMMA sphere, 40 kV ISO "narrow" X-ray field.

angle of incidence	$H_p(10,\alpha)/H_p(10,0^o)$ 40 kV,	calculated Pernicka (1991)	calculated Grosswendt (1988)	calculated Dimbylow (1988)
0°	1.000+/-0.001	1.0	1.0	1.0
30°	0.971+/-0.009		0.944	0.951
45°	0.915+/-0.009			
60°	0.825+/-0.019	0.817	0.735	0.786
90°	0.309+/-0.020	0.316	0.271	0.320
120°		0.023		
150°		0.003		
180°		0.001		

Table IIIb The same as a) but for 80 kV and 295 keV respectively.

angle of incidence	$H_p(10,\alpha)/H_p(10,0^o)$ 80 kV	calculated **Pe**rnicka (1991)	calculated Grosswendt (1988)	calculated Dimbylow (1988)
0°	1.000+/-0.004	1.0	1.0	1.0
30°	0.959+/-0.009		0.966	0.959
45°	0.937+/-0.004	0.931		
60°	0.862+/-0.021	0.845	0.832	0.840
90°	0.467+/-0.017	0.454	0.453	0.488
120°	0.108+/-0.003	0.112		
150°	0.044+/-0.001	0.037		
180°				
angle of incidence	$H_p(10,\alpha)/H_p(10,0^o)$ 295 kV	calculated Pernicka (1991)	calculated Grosswendt (1988)	calculated Dimbylow (1988)
0°	1.000+/-0.007	1.0	1.0	1.0
30°	0.992+/-0.025		0.986	0.989
45°				
60°	0.914+/-0.015	0.927	0.918	0.942
90°	0.627+/-0.016	0.631	0.645	0.689
120°	0.214+/-0.006	0.229		
150°	0.100+/-0.002	0.092		
180°	0.088+/-0.002	0.072		

Table IIIc The angular dependence factor H_p (10,α)/ H_p(10,0°) for a PMMA sphere irradiated in a ^{137}Cs γ field.

angle of incidence	H_p (10,α)/ H_p(10,0°) 662 kV	calculated Grosswendt (1988)	calculated Dimbylow (1988)
0°	1.000+/-0.008	1.000	1.000
30°	0.9940.011	0.995	1.005
60°	0.992+/-0.010	0.955	0.988
90°	0.748+/-0.020	0.780	0.814
120°	0.379+/-0.009		
150°	0.212+/-0.004		
180°	0.166+/-0.003		

The angular dependence factors collected in the Tables above are shown in Figs 7 a-d. The experimental results are shown with error bars together with calculated values from Grosswendt (1988).

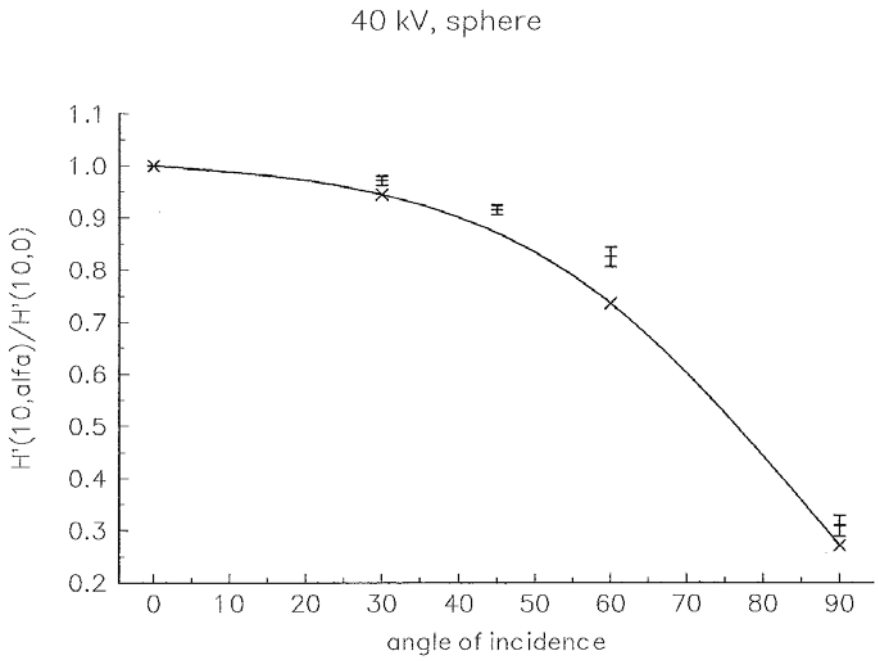

Fig 7 a. H'(10,α/H'10,0°) for a sphere irradiated in a 40 kV X-ray field, (-) with error bars are experimental values, (x) connected with a solid line are calculated values from Grosswendt (1988).

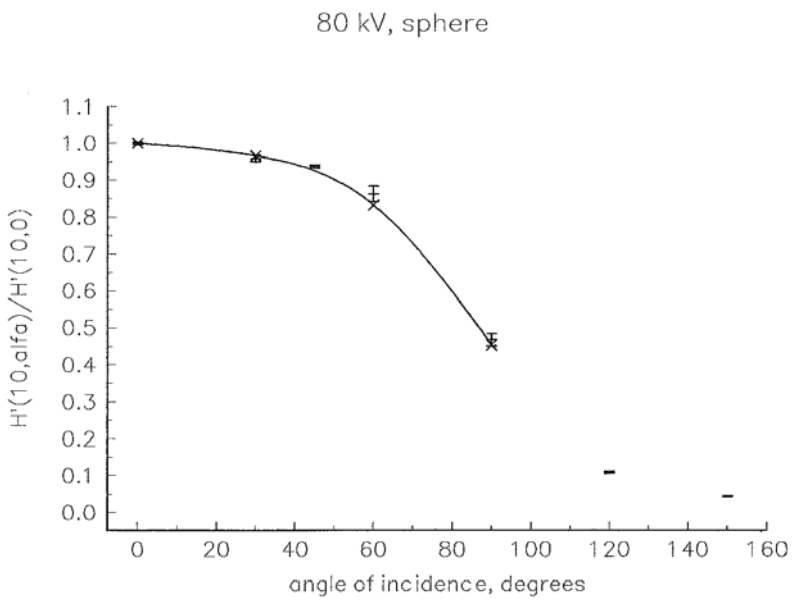

Fig 7 b. The same as a) but for 80 kV.

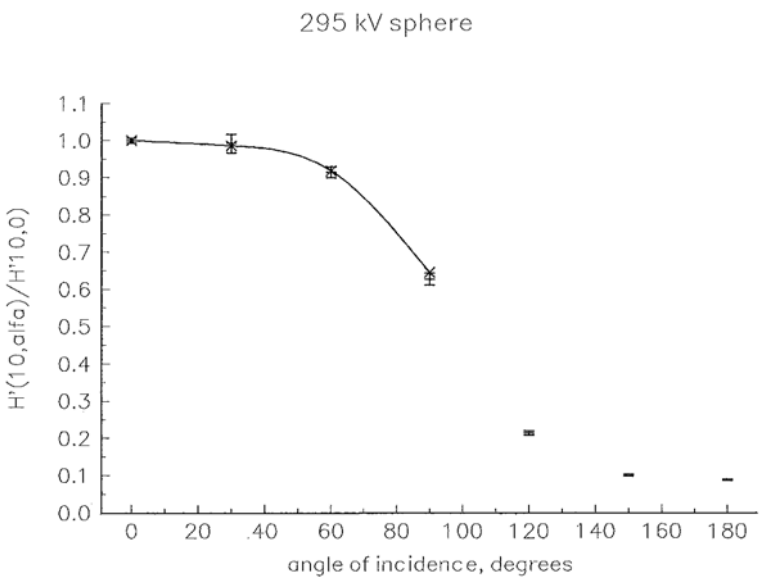

Fig 7c the same as a) but for 295 kV

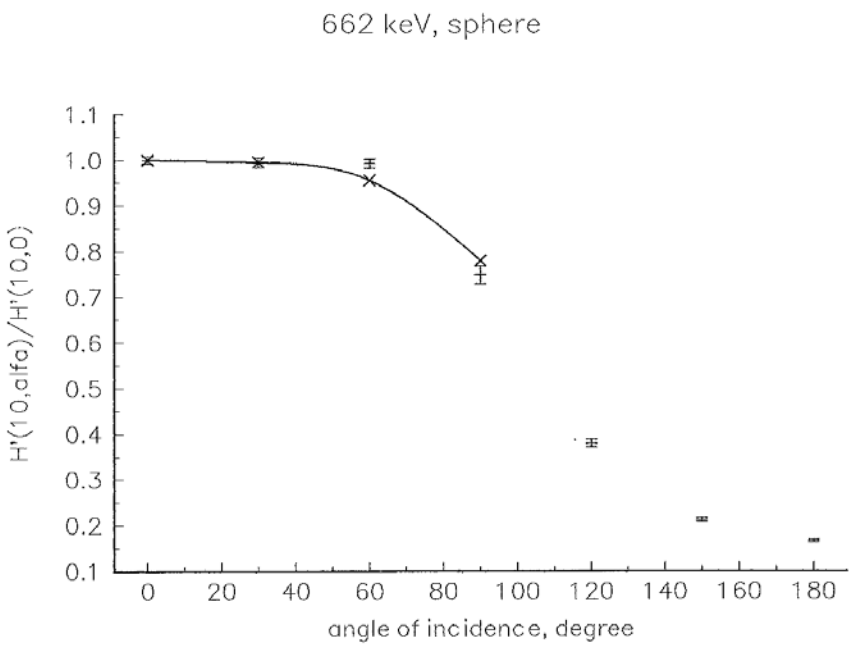

Fig 7 d. The same as a) but for 662 keV ^{137}Cs γ-rays.

The experimental are in good agreement for all X-ray qualities except for 40 kV where there exists a discrepancy. It is, however, obvious from Table 3 a that the experimental values are in better agreement with calculated values from Pernicka(1991) and in some cases lower than the values by Dimbylow(1988)

Table IV a and b. H'(10,α)/H'(10,0^{o}) determined for 40 kV, 80kV 295kV ISO "narrow" X-ray beams and 662 keV,^{137}Cs γ-rays. The experimental values are compared with calculated values by Grosswendt (1992).

angle of incidence	40 kV E_{eff} 32 keV	Calculated Grosswendt (1992)	80 kV E_{eff} 64 keV	Calculated Grosswendt (1992)
0°	1.000 +/- 0.016	1.000	1.000+/-0.010	1.000
30°	0.974 +/- 0.011	0.957	0.958+/- 0.020	0.960
60°	0.778 +/-0.015	0.752	0.840+/-0.050	0.760
70°	0.595 +/-0.030		0.694+/-0.028	
75°		0.469		0.506
80°	0.303+/-0.021		0.450+/-0.015	
82.5^{o}		0.213		0.275
90°	0.034+/-0.001	0.001	0.131+/-0.001	0.015
120°		0.005	0.140+/-0.004	0.061
150°		0.022	0.192+/-0.005	0.117
180°	0.053+/-0.001	0.035	0.250+/-0.020	0.228

angle of incidence	295 kV E_{eff} 248 keV	Calculated Grosswendt (1992)	662 keV	Calculated Grosswendt (1992)
0°	1.000±0.012	1.000	1.000±0.0.16	1.000
30°	0.964±0.035	0.986	0.979±0.029	0.99
60°	0.887±0.035	0.886	0.966±0.015	0.952
70°	0.838±0.038		0.926±0.016	
75°		0.681		0.819
80°	0.623±0.050			
82.5°		0.430		0.586
90°	0.228±0.005	0.014	0.324±0.010	0.009
120°	0.228±0.017	0.060	0.352±0.004	0.049
150°	0.251±0.004	0.260		0.394
180°	0.349±0.007	0.340		0.486

The angular dependence factor for the 30x30x15 cm^3 PMMA slab phantom is experimentally determined using the same technique as for the sphere. The experimental results are shown in Table 4a) and b) together with calculated factors of Grosswendt (1992).

The experimental values of H'(10,α)/ H'(10,0°) for a PMMA slab are shown with error bars, one standard deviation) together with calculated values (crosses connected with a solid line) by Grosswendt (1992) in Figs 8 a - d.

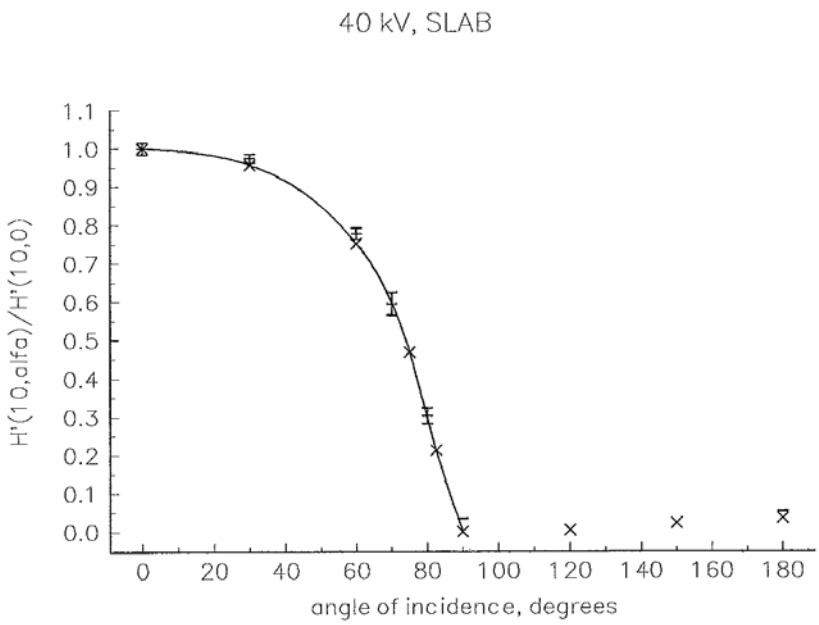

Fig 8a. The angular dependence factor plotted as a function of angle of incidence for a 40 kV X-ray field on a PMMA slab phantom. with error bars and calculated values - Experimental values -x

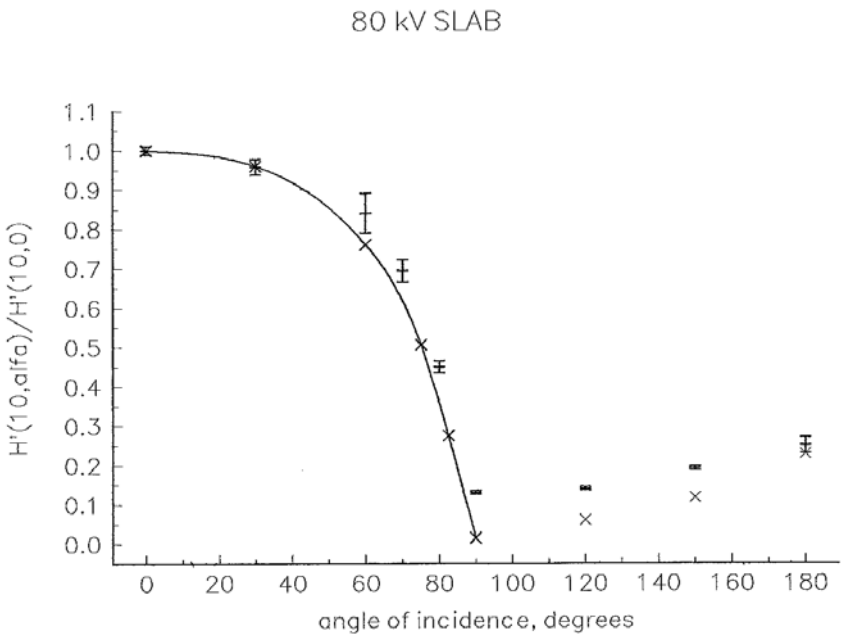

Fig 8 b. The same as a) but for 80 kV

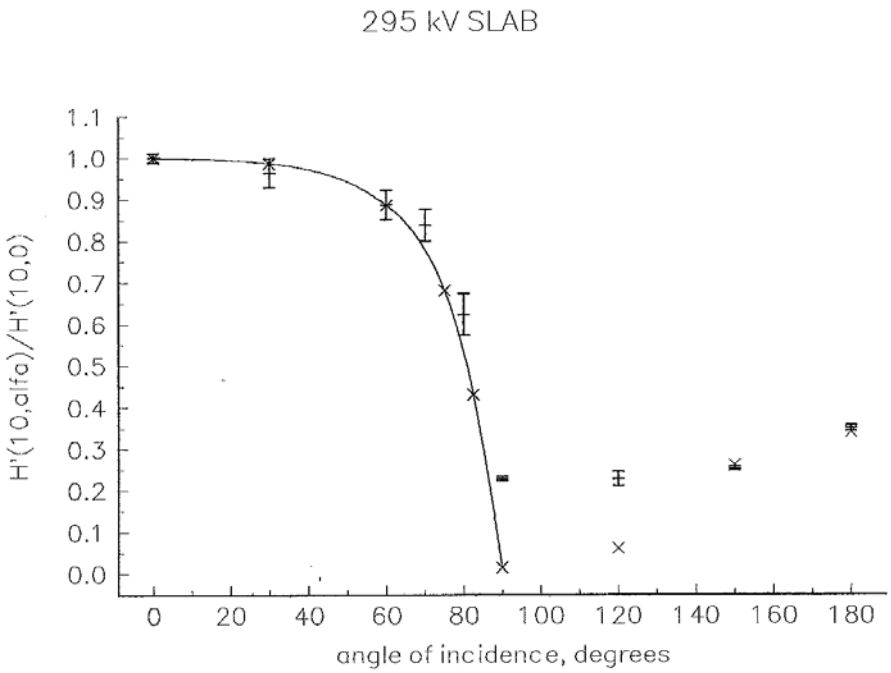

Fig 8c. The same as a) but for 295 kV.

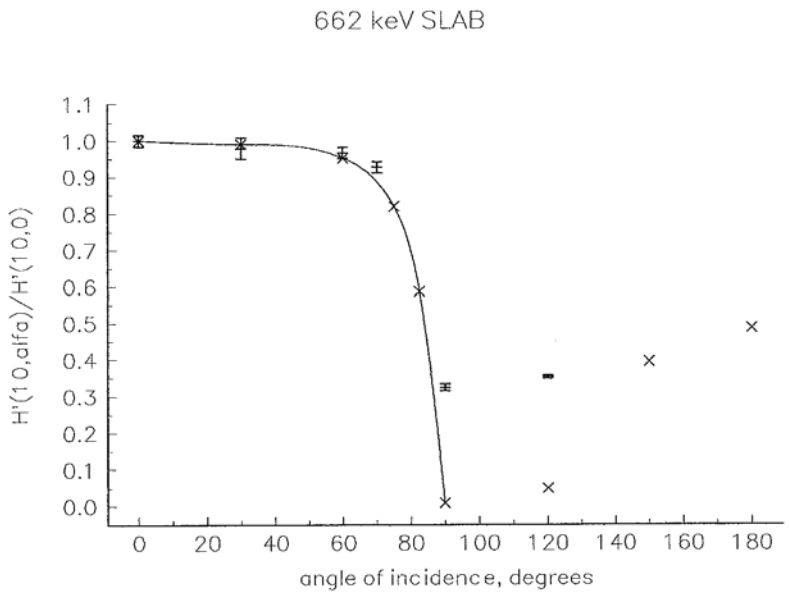

Fig 8d. The same as a) but for ^{137}Cs, 662 keV photons.

For all beam qualities except 40 kV the experimental values for H'(10,α)/H'(10,0^{o}) are significantly higher than the calculated ones for angles of incidence > 60°.The irradiations are performed in a crowded and quite narrow room at the Standard Laboratory for Dosimetry and it is obvious that some of the high experimental values are caused by scattered radiation from the environment and the air. An indication for this is that the experimental value for 40 kV at 90° is not zero which is expected from Monte Carlo calculations. Some of the measurements have also been repeated in Prague in a more spacious room resulting in values for H'(10,α)/H'(10,0^{o}) which are one fifth of those obtained for angles >90° at Stockholm.

This can however not explain all differences.The discrepancy between calculated and measured values does not appear in the measurements on the sphere and only for larger angles of incidence on the slab phantom. That means that the differences appear when the primary photons are attenuated in quite a large amount of PMMA before reaching the dosemeters. As seen from Fig 9, the surface of the sphere is curved so that the primary photons are not attenuated so much as when the primary photons have to be transported through 5 - 15 cm of PMMA which is the case for larger angles of incidence on the slab phantom. We must bear in mind that the Monte Carlo calculations are performed for the phantom material in vacuum (Grosswendt 1991).The comparatively large amount of scattered radiation from the surrounding air together with a strongly attenuated primary fluence might give an explanation to the discrepancies. The amount of phantom material in the vicinity of the dosemeters for the slab geometry will also result in a higher ratio between scattered and primary radiation.

In order to explain these discrepancies it is our intention to perform Monte Carlo calculations and determine the ratio between primary and scattered radiation at the dosemeter position when the slab phantom is surrounded by air. It is also important to determine the effective energy for the spectrum at the measuring position inside the PMMA phantom for large angles of incidence compared to the situation for normal incidence. If the ratio between

primary and scattered photons has changed considerably the effective energy might decrease so much that the assumption that the detector response is the same for all angles of incidence is not true.

5. Discussion

5.1 Corrections due to choice of calibration phantom.

The ICRU sphere is for many reasons impractical for calibration of more than one individual dosimeter at a time. For this reason a slab phantom seems to be much more useful. The question arises how large is the influence from the phantom geometry on the calibration factor.

As pointed out by Wagner (1989) there are two different points of view.

a) *The metrologically rigorous approach.* When another shape and composition of the phantom material is used, corrections must be applied in the calibration procedure for the deviation in detector signal from that expected for the expanded field on the ICRU sphere.

b) *The empirical method.* Phantoms other than the ICRU sphere but sufficiently anthropomorphic for the radiation of interest are used and a calibration factor is obtained taking the conversion factor for the directional dose equivalent directly.'

An extensive set of conversion factors from the ICRU sphere to other types of phantoms is now available (Grosswendt 1991). Therefore the empirical approach is recommended. The calibration results for phantoms with backscatter characteristics comparable with the ICRU sphere should give calibration results with accuracies well within the guidelines given by ICRU and ICRP (see the Introduction). .

The Monte Carlo calucations performed in order to derive conversion factors indicate that the extra mass in the first cm for the slab results in a larger region that contributes to the dose equivalent by secondary radiation than the same region for a 30 cm sphere, see fig.9 (Hertel1990). The possible effect on the calculations is discussed in Sect 4.

The difference in the angular dependence factors between a spherical and a slab phantom is rather small which is seen by comparison between the Figures 7 and 8 a - d respectively. In fact a calibration on a slab phantom will probably simulate the situation for an individual dosemeter placed on the breast better than a calibration on a sphere.

5.2 Possibilities to underestimate the radiation risk in personal monitoring.

The effective dose equivalent, E, is designed to be the quantity to which the radiation risk is related. It is then of interest to compare the measured personal dose equivalent, $H_p(10)$, with E. Both E and $H_p(10)$ are varying with the direction of the incident radiation. Zankl, Petoussi and Drexler (1992) has in a horizontal and parallel field determined the quotient of effective dose to air kerma free in air E/K_{air} as a function of photon energy for different angles of incidence.; $\alpha = 0^o$ (a.p.), $\alpha = 90^o$ (l lat.), $\alpha = 180^o$ (p.a.), $\alpha = 270^o$ (r lat.) and a full 360° rotation around the longitudinal axis. Grosswendt (1991) has calculated the ratio Hp(10)/Kair also as a function of photon energy and angle of incidence. Data from these investigations are collected together with the present experimental values in Table 5a and b. for a) $\alpha = 0^o$ and b) $\alpha = 180^o$.

Table V a and b. The ratio between the personal dose equivalent and air kerma for a PMMA slab and for ICRU tissue slab from Grosswendt (1991) are used together with the ratio between effective dose and air kerma from Zankl.et al. (1992). The deduced values from the present experiments are listed in the last column.

energy keV	$E(0^o)/K_a$	$H_p(10,0^o)/K_a$ tissue	$H_p(10,0^o)/K_a$ PMMA	$E(0^o)/H_p(10,0)$ tissue	$E(0^o)/H_p(10,0)$ PMMA	exp.
10	0.065	0.0097	0.0645	6.73	1.01	
15	0.040	0.268	0.430	0.149	0.09	
25	0.251	0.879	1.045	0.286	0.240	
32	0.879	1.105	1.310	0.382	0.323	0.353
35	0.594	1.300	1.449	0.457	0.410	
50	1.111	1.769	1.963	0.628	0.566	
60	1.306	1.890	2.070	0.691	0.626	
64	1.353		2.076		0.652	0.64
70	1.424	1.911	2.085	0.745	0.683	
80	1.433	1.891	2.035	0.758	0.704	
100	1.397	1.812	1.909	0.771	0.732	
150	1.249	1.650	1.663	0.781	0.751	
200	1.172	1.489	1.528	0.787	0.762	
242	1.136	1.439	1.472	0.789	0.771	0.80
300	.087	1.370	1.394	0.793	0.779	
500	1.043	1.256	1.269	0.830	0.822	
662	1.031	1.221	1.239	0.844	0.832	0.82
1000	1.003	1.175	1.180	0.855	0.850	

Table V b

energy keV	E(180°)/Ka	H_p(10,180°)/ K_{air} tissue	H_p(10,180°)/ K_{air} PMMA	tissue	E(180°)/ H_p(10,180°) PMMA	exp.
10	0.0025	0	0	-	-	
15	0.0058	0	0	-	-	
25	0.056	0.00265	0	21.2	-	
32	0.187	0.083	0.056	4.03	3.34	2.53
35	0.237	0.153	-	2.30	2.00	
50	0.641	0.320	0.336	2.00	1.91	
60	0.853	0.442	0.449	1.93	1.90	
64	0.902	0.467	0.467	1.93	1.93	1.70
70	0.981	0.505	0.496	1.94	1.98	
80	1.020	0.543	0.519	1.88	1.97	
100	1.028	0.545	0.513	1.89	2.00	
150	0.966	0.549	0.491	1.76	1.96	
200	0.926	0.557	0.492	1.66	1.88	
242	0.910	0.569	0.502	1.60	1.81	1.82
300	0.888	0.586	0.516	1.52	1.72	
500	0.880	0.642	0.569	1.37	1.55	
1000	0.919	0.721	0.660	1.23	1.39	

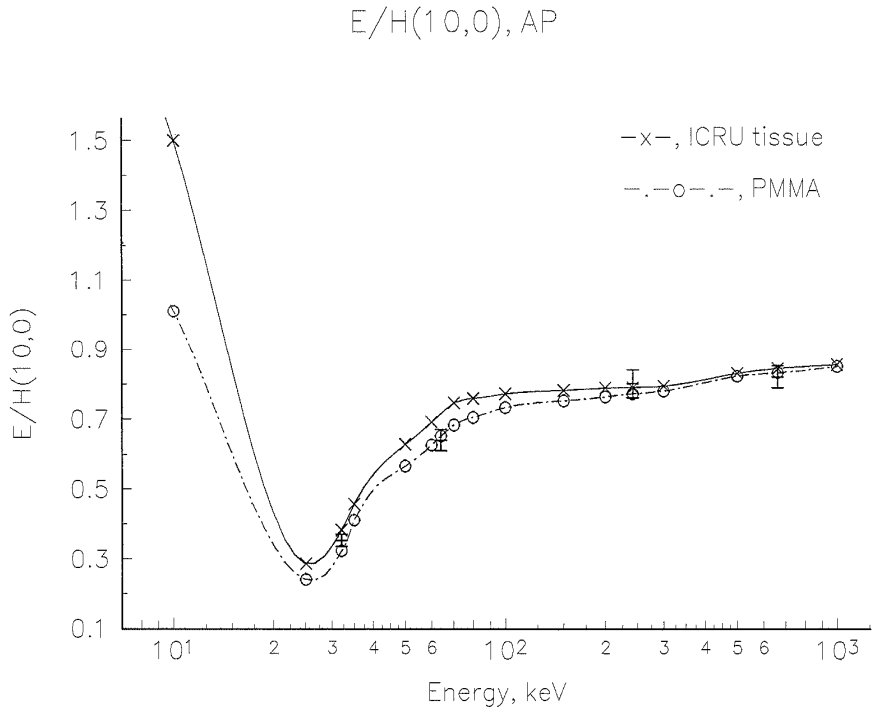

Fig 9.Tthe resulting ratio E(0°)/Hp(10,0°) for PMMA and ICRU tissue together with deduced results from experiments shown with error bars.

Fig 10 shows E(α)/Hp(10,α) received from :

$$\frac{E(\alpha)}{H_p(10,\alpha)} = \frac{E(\alpha)}{K_{air}} \cdot \frac{K_{air}}{H_p(10,\alpha)} \qquad (10)$$

From Fig 10 can be seen that with an a.p. irradiation ($\alpha = 0^o$) $E/H_p(10)$ is always < 1, that is $H_p(10,0^o)$ is overestimating E except for energies very near and below 10 keV.

At lateral incidence of the radiation $H_p(10,\alpha)$ might underestimate the radiation risk (E) as well as for $\alpha=180^o$ at PA incidence. The situation is however not so bad since normally the individual dosemeter is worn outside the clothing and the dosemeter will give a registration from the radiation which has not been attenuated in a large amount of material which is the case when measured inside a slab phantom. However, the main error source in measuring $H_p(10,\alpha)$ or estimating E(α) is when the incident radiation is inhomogenously distributed over the body, Sievert (1963).

Acknowledgements

We would like to thank Ass Prof. Lennart Lindborg at SSI for many valuable discussions and the staff of the Dosimetry laboratory Olle Gullberg and Göran Samuelsson, for excellent help with the irradiation equipment and fabrication of the phantoms. We also want to thank Åsa Carlsson for her excellent assistance during the preparation and read out of the dosemeters and during the long time irradiations at Stockholm. Prof Gudrun Alm Carlsson is gratefully acknowledged for her interest in this work and valuable comments on the manuscript.

References

Bartlett, DT., Francis, T., M. and Dimbylow, P., J. (1989) *Methodology for the Calibration of Photon Personal Dosemeters: Calculation of phantom Backscatter and Depth Dose Distributions.* Rad. Prot. Dosim. **27**, pp 231-244.

Burns (1958) *Conversion of Depth Doses from one FSD to another.* Brit J Radiology **31**,p 643.

da Rosa, L., A., F. and Nette, H., P. (1988), ,Int J Radiat. Appl. Instr., Part A, Appl. Radiat. Isot. **39,** No 3, p 191-197.

Dimbylow P., J. (1989) *Calibration of Photon Personal Dosemeters in Terms of the ICRU Operational Quantities: Calculcation of Phantom backscatter and Depth-Dose Distributions,* NRPB-R230, Chilton, Didcot, UK.

Grosswendt, B., Hohlfeld,K., Kramer, H.,M., and Selbach H-J, (1988) *Conversion Factors for ICRU Dose Exuivalent Quantities for the Calibration of Radiation Protection Dosemeters.* PTB-Dos 11e (transation).

Grosswendt, B., Hohlfeld,K., Kramer, H.,M., and Selbach H-J, (1988) *Conversion Factors for ICRU Dose Exuivalent Quantities for the Calibration of Radiation Protection Dosemeters.* PTB-Dos 11e (transation).

Grosswendt, B. (1991) *The Angular Dependence and Irradiation Geometry Factor for the Dose Equivalent for Photons in Slab Phantoms of Tissue-Equivalent Material and PMMA.* Radiat. Prot. Dosim. **35**, 4, pp 221-235.

Grosswendt B (1992) *Coefficients for the Conversion of Air Collision Kerma to Dose Equivalent for the Calibration of Individual Dosemeters in X-ray Fields..* Radiat. Prot. Dosim. **40,**3, pp 169-184.

Hertel, N.E. and McDonald, J.C.,(1990) *Methods for the Calibration of Photon Personel Dosemeters in Terms of the Ambient Dose Equivalent.* Radiat. Prot. Dosim. **32**, 3 pp 149-156.

IAEA, 1988, *Calibration of Radiation Protection monitoring Instruments,*Vienna.

ICRP 35 (!982) International Commission on Radiological Protection, *General Principles of Monitoring for Radiation Protection of Workers,* ICRP publication 35, Annals of the ICRP **9**, No4 (Pergamon Press, Oxford).

ICRP 60(1991), International Commission on Radiological Protection, *1990 Recommendations of the the International Commission on Radiological Protection,* ICRP Publication 60, Annals of the ICRP **21**, No 1/3 (Pergamon Press, Oxford)

ICRU 33, (1980) *Radiation Quantities and Units.* Report 33 (Washington, DC 20014: ICRU Publications).

ICRU 39, (1985) *Determination of Dose Equivalents Resulting from External Radiation Sources.* Report 39. (Bethesda, MD 20814: ICRU Publications).

ICRU 47.(1992) *Measurement of Dose Equivalents from External Phioton and Electron Radiations.* Report 47. (Bethesda, MD 20814)

ISO (1979), International Standards Organization, *X and gamma Reference Radiations for Calibrating Dosemeters and Doseratemeters and for Determining their Response as a Function of Energy.*International Standard ISO 4037.

Johns, H., E., Bruce W., R., and Reid, W., B. (1958). *The Dependence of Depth Dose on Focal Skin Distance.* Brit. J Radiol **31**, p 254-260.

Pernicka, F,(1991), *Monte Carlo Calculations of the Air Kerma to H'(10,□) for a PMMA Slab Phantom,*(Private Communication)

Perroche A. -M and Boutillon M, *Measurement of Ambient Dose Equivalent and Directional Dose Equivalent in a Co-60 beam* ,Radiat. Prot. Dosim. **27**, 3 pp 139-148.

Sievert, R., M. (1963) *Method of Recording Individual Doses and Dose Rates during Radiation Work.* Proc. Symposium on personal dosimetry techniques for external radiation. OECD, European Nuclear Energy Agency pp 173-188.

Wagner, S., R.(1989) *Freedom of Phantom Choice in Calibrating Individual Monitors - Consequences and Restrictions.* Radiat. Prot. Dosim. **28**, no12, p 59-61.

Wernli, C., Jossen, H and Valley, J-F, 1989, *Methods of Measurement and Calibration in Personal Dosimetry for External Radiation: Presentation of the Concept and the results of a Test Programme in Switzerland.* Radiat. Prot. Dosim. **28**, p157-160.

Will, W., (1989) *Measurement of Conversion Coefficients for estimating Photon Individual Dose Equivlents for a Cuboid Water Phantom.* Radiat. Prot. Dosim. **27,** no 1, p 9-14.

Will, W. (1991) *Measurement of conversion Coefficients for calibrating Idividual Dosemeters with Respect to the Operational Dose Quantities on the PMMA Slab Phantom.Radiat. Prot. Dosim.*

Zankl, M., Petoussi,N., and Drexler G. (1992) *Effective Dose and Effective Dose Equivalent-The Impact of the new ICRP Definition for external Photon Radiation.* Health Physics, **62**, 5, p395-399.